



Experimental and Numerical Study of Collector Geometry Effect on Solar Chimney Performance

Aseel K. Shyaa* Rafea A. H. Albaldawi**

Maryam Muayad Abbood***

*, **, ***Department of Mechanical Engineering/ University of Al-Mustansiriyah

*Email: aseelkhshyaa@yahoo.com

**Email: rafa_a70@yahoo.com

***Email: memomoaed@yahoo.com

(Received 18 February 2016; accepted 5 May 2016)

<http://dx.doi.org/10.22153/kej.2016.05.002>

Abstract

There have been many advances in the solar chimney power plant since 1930 and the first pilot work was built in Spain (Manzanares) that produced 50 KW. The solar chimney power plant is considered of a clean power generation that needs to be investigated to enhance the performance by studying the effect of changing the area of passage of air to enhance the velocity towards the chimney to maximize design velocity. In this experimental and numerical study, the reduction area of solar collector was investigated. The reduction area that mean changing the height of glass cover from the absorbing plate ($h_1=3.8\text{cm}$, $h_2=2.6\text{cm}$ and $h_3=1.28\text{cm}$). The numerical study was performed using ANSYS Fluent software package (version 14.0) to solve governing equations. The aim of this work was to study the effect of change the height of reduction area to the design velocity (velocity move the blade of turbine at inlet in the chimney). The results showed that the third height ($h_3=1.28\text{cm}$) gives the best result because when decreasing the height between the glass cover and absorbing plate, the area between them decreased and the design velocity increased then the efficiency of solar chimney model was increased.

Keyword: Solar chimney, Collector, Mathematical modeling, Numerical simulation, Enhance performance.

1. Introduction

The solar chimney power plant consists of a solar air collector, a solar chimney and a turbine coupling with generator [1]. The main aim from manufacture the solar chimney power plant to convert the power of solar radiation energy to thermal energy and by the rotation of turbine convert to mechanical energy and put the electric station in this to generate the electrical energy that's used in different way in the life. The solar chimney power plant is shown in Figure (1). The change of area is use to generating swirl flow inside solar collector of the solar chimney. Mark[2] The height of the roof inlet was adjustable, so that the ratio of flow areas between

roof inlet and roof outlet could be varied. The reduction in pressure at the point of reduction area is come from the reduction in area which will draw the air flow to the region of area after the reduction. This technique could be utilized to increase heat transfer between the air flow and absorber plant and between air flow and glass cover, and to increase air velocity. Atit [3] constructed four small-scale physical models of the solar chimney were constructed. The height of the roof inlet was adjustable, so that the ratio of flow areas between roof inlet and roof outlet could be varied. In addition, there were plants with constant cross sectional area towers and a plant with a divergent tower. Also there was one plant with a novel roof shape. Results indicate that the

flow power increases with the decrease in the ratio of flow areas between roof inlet and roof outlet. The divergent chimney also results in significant increase in flow power compared to that of the constant area chimney. It was observed that the system with the proposed novel roof shape provides approximately the same performance as the conventional shaped system, while the ratio of flow areas between roof inlet and roof outlet for the novel system could be practically reduced. Correspondingly the increase in performance to some specific value which is much lower than the typical system could be achieved. The experimental results are different from the predicted values, but show the same trends.

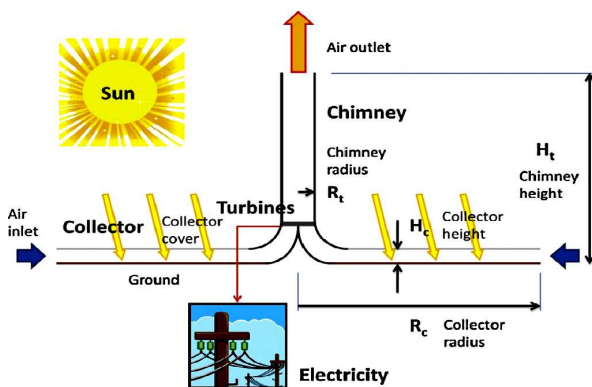


Fig. 1. Solar chimney power plant [4].

2. Mathematical Model

The mathematical model analyzes the flow field inside solar chimney model fig (2), using the governing equations. The following assumptions have been considered in mathematical model:-

1. A steady state condition is assumed, which is an approximation because solar radiation is transient in real conditions.
2. The working air in tests proceedings as an incompressible fluid.
3. The properties of working air in all tests such as the coefficient of viscosity and the thermal conductivity are constant.
4. The working air behaves as an ideal gas.
5. Both the solar collector and chimney tower are insulated to avoid heat losses to the environment.
6. Air enter to the solar chimney is by natural convection.
7. The flow in the collector is considered as a flow between two parallel plates.
8. The flow is assumed one-dimensional between the collector inlet and the turbine inlet. In the chimney tower the flow is assumed one

dimensional between the turbine outlet and the tower outlet.

9. The flow through collector section has complete symmetry with the θ direction, so $\frac{\partial}{\partial \theta} = 0$, and there is no flow in the θ and z - directions ($v_\theta, v_z = 0$).
10. The flow through chimney section has complete symmetry with the θ direction, so $\frac{\partial}{\partial \theta} = 0$, and there is no flow in the θ and r - directions ($v_\theta, v_r = 0$).

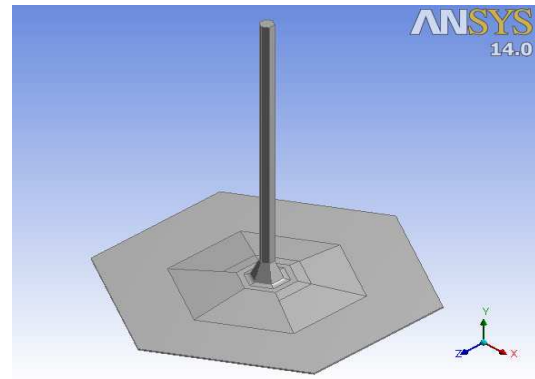


Fig. 2. Solar chimney model.

Continuity equation [5]

$$\frac{\partial(\rho v_r)}{\partial r} + \frac{\partial(\rho v_z)}{\partial z} + \frac{1}{r} \frac{\partial(\rho v_\theta)}{\partial \theta} + \frac{\rho v_r}{r} = 0 \quad \dots(1)$$

For collector:-

$$\rho \frac{\partial v_r}{\partial r} + \rho \frac{v_r}{r} = 0 \quad \dots(2)$$

For chimney:-

$$\rho \frac{\partial v_z}{\partial z} = 0 \quad \dots(3)$$

Momentum equation [5]:-

For collector:-

$$\rho \cdot v_r \frac{\partial v_r}{\partial r} + \frac{\partial P}{\partial r} - \mu \left[\frac{4}{3} \left(\frac{\partial^2 v_r}{\partial r^2} + \frac{1}{r} \frac{\partial v_r}{\partial r} - \frac{2 v_r}{r^2} \right) + \frac{\partial^2 v_r}{\partial z^2} \right] = 0 \quad \dots(4)$$

For chimney:-

$$\rho v_z \frac{\partial v_z}{\partial z} - g \rho \beta (T - T_a) - \mu \left[\frac{4}{3} \frac{\partial^2 v_z}{\partial z^2} + \frac{1}{r} \frac{\partial v_z}{\partial r} + \frac{\partial^2 v_z}{\partial r^2} \right] = 0 \quad \dots(5)$$

Energy equation[5]:-

For collector

$$\begin{aligned}
 &k \left[\frac{\partial^2 T}{\partial r^2} + \frac{1}{r} \frac{\partial T}{\partial r} + \frac{\partial^2 T}{\partial z^2} \right] \\
 &+ 2\mu \left[\left(\frac{\partial v_r}{\partial r} \right)^2 + \left(\frac{v_r}{r} \right)^2 \right. \\
 &+ \left. \frac{1}{2} \left(\frac{\partial v_r}{\partial z} \right)^2 - \frac{1}{3} \left(\frac{\partial v_r}{\partial r} + \frac{v_r}{r} \right)^2 \right] + v_r \frac{\partial \rho}{\partial r} \\
 &- \rho C_p \left[v_r \frac{\partial T}{\partial r} \right] \\
 &= 0 \qquad \dots (6)
 \end{aligned}$$

For chimney

$$\begin{aligned}
 &k \left[\frac{\partial^2 T}{\partial r^2} + \frac{1}{r} \frac{\partial T}{\partial r} + \frac{\partial^2 T}{\partial z^2} \right] \\
 &+ 2\mu \left[\frac{2}{3} \left(\frac{\partial v_z}{\partial z} \right)^2 + \frac{1}{2} \left(\frac{\partial v_z}{\partial r} \right)^2 \right] \\
 &+ v_z \frac{\partial \rho}{\partial z} - \rho C_p \left[v_z \frac{\partial T}{\partial z} \right] \\
 &= 0 \qquad \dots (7)
 \end{aligned}$$

2.1. Mathematical Model in the Collector

The energy balance equations for the glass cover, the absorber plate and the airflow in the collector are given in the following equation respectively [6].

For the glass cover

$$U_t(T_a - T_c) + h_{r,p-c}(T_p - T_c) + h_1(T_f - T_c) = 0 \qquad \dots (8)$$

For the absorber plate

$$\begin{aligned}
 S + U_b(T_a - T_p) + h_2(T_f - T_p) \\
 + h_{r,p-c}(T_c - T_p) \\
 = 0 \qquad \dots (9)
 \end{aligned}$$

For the airflow in the collector

$$h_1(T_c - T_f) + h_2(T_p - T_f) = q_u \qquad \dots (10)$$

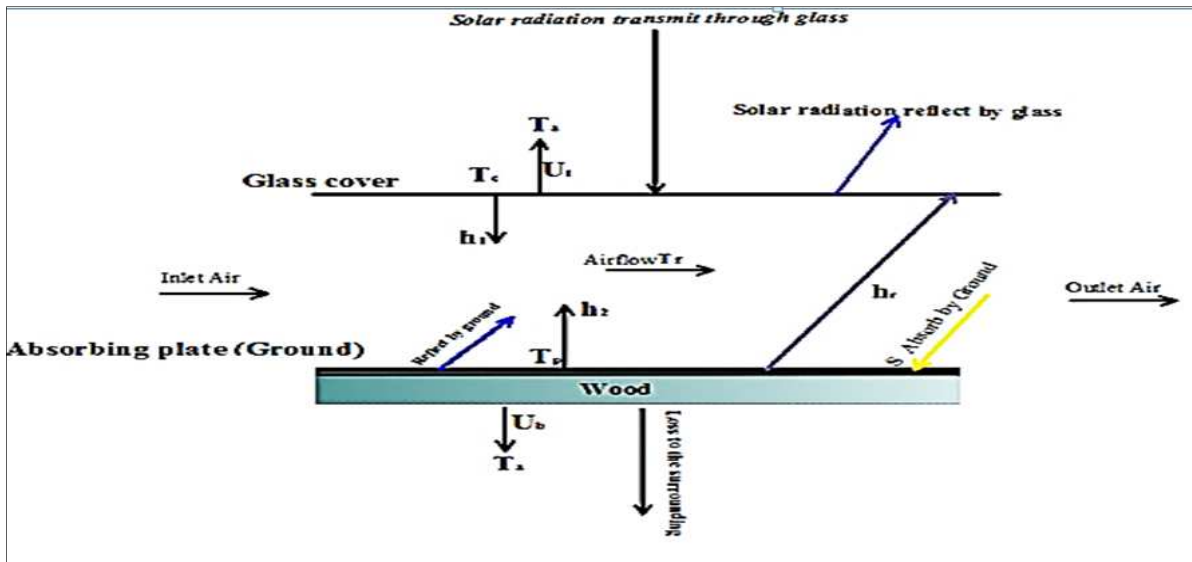


Fig. 3. Heat transfer scheme of solar collector.

The solar radiation absorbed by the absorber plate

$$\begin{aligned}
 \text{is} \\
 S = I_T \alpha_p \tau \qquad \dots (11)
 \end{aligned}$$

where:-

I_T : Solar incidence on the surface of absorber plate W/m^2

α_p : Absorber plate absorptivity

τ : Glass transmittance

The mean temperature of airflow can be given by [7]:-

$$T_f = \frac{(T_{f,i} + T_{f,o})}{2} \qquad \dots (12)$$

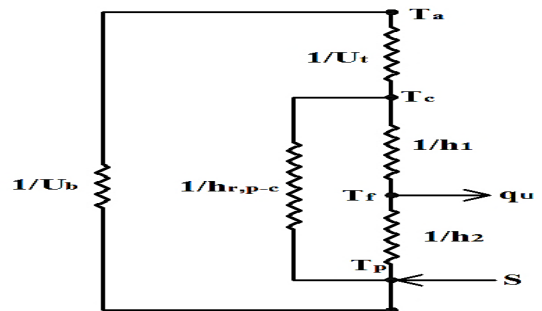


Fig. 4. Thermal network for the collector of solar chimney.

The cover glass temperature is found from equation [6]:-

$$T_c = T_p - \frac{U_t (T_p + T_a)}{h_{p-c} + h_{r,p-c}} \quad \dots (13)$$

h_{p-c} : Convection heat transfer coefficient between the absorber plate and the glass cover is given by:-

$$Nu = \frac{h_{p-c} \times L}{k} \quad \dots (14)$$

where:

L : The spacing between the absorber plate and the glass cover, m

k : Thermal conductivity of air $W/m K$

Nu : The value of Nusselt number could be obtained using the expression [8]:-

$$Nu = 0.54 Ra^{1/4} \quad \text{For } 10^4 \leq Ra \leq 10^7 \quad \dots (15)$$

$$Nu = 0.14 Ra^{1/3} \quad \text{For } 10^7 \leq Ra \leq 10^{11} \quad \dots (16)$$

where:

Ra : Rayleigh number and is given by:-

$$Ra = Gr Pr = \frac{g\beta\Delta T_{p-c} L^3}{\nu \alpha} \quad \dots (17)$$

g: Gravitational acceleration m/s^2

β : Volumetric thermal expansion coefficient of air K^{-1}

α : Thermal diffusivity m^2/s

ΔT_{p-c} : The temperature difference between the absorber plate and the glass cover

$h_{r,p-c}$: Radiation heat transfer coefficient between the absorber plate and the glass cover. It could be calculated as suggested [6]:-

$$h_{r,c-p} = \frac{\sigma (T_c + T_p)(T_c^2 + T_p^2)}{\left(\frac{1}{\epsilon_p} + \frac{1}{\epsilon_c} - 1\right)} \quad \dots (18)$$

The overall top heat loss coefficient from the glass cover to the ambient obtained from empirical equation as follows [6]:-

$$U_t = \left\{ \frac{N}{\frac{c}{T_p} \left[\frac{(T_p - T_a)^e}{(N-f)} \right]} + \frac{1}{h_w} \right\}^{-1} + \frac{\sigma (T_p^2 + T_a^2)(T_p + T_a)}{(\epsilon_p + 0.00591 N h_w)^{-1} + \left[\frac{2N + f - 1 + 0.133 \epsilon_p}{\epsilon_c} \right] - N} \quad \dots (19)$$

where:

h_w : The convective heat transfer coefficient due to the wind is estimated as suggested by [6]:-

$$h_w = 2.8 + 3 V \quad \dots (20)$$

V : The wind speed m/s

N = number of glass covers

$$f = (1 + 0.089h_w - 0.1166h_w\epsilon_p)(1 + 0.07866 N)$$

$$c = 520 (1 - 0.000051 \beta^2)$$

for $0^\circ < \beta < 70^\circ$. for $70^\circ < \beta < 90^\circ$, use $\beta = 70^\circ$
 β = collector tilt (degrees)

$$e = 0.43 \left(1 - \frac{100}{T_p} \right)$$

The back loss coefficient U_b is given as [6]:-

$$U_b = \frac{k}{\delta} \quad \dots (21)$$

where k insulator thermal conductivity and δ thickness.

The collector overall loss coefficient, U_L is given by [6]:-

$$U_L = \frac{(U_t + U_b)(h_1 h_2 + h_1 h_{r,p-c} + h_2 h_{r,p-c}) + U_b U_t (h_1 + h_2)}{h_1 h_{r,p-c} + h_2 U_t + h_2 h_{r,p-c} + h_1 h_2} \quad \dots (22)$$

Where:

h_1 : Convection heat transfer coefficient between the glass cover and the airflow.

h_2 : Convection heat transfer coefficient between the absorber plate and the airflow.

h_1 and h_2 can be assumed to be equal and can be evaluated from the following equation:-

$$h_1 \text{ or } h_2 = Nu \frac{k}{D_h} \quad \dots (23)$$

where Nu is given by

$$Nu = 0.0158 Re^{0.8} \quad \dots (24)$$

$$R = \frac{\dot{m} D_h}{A_c \mu} \quad \dots (25)$$

The collector efficiency factor F' is found from the equation [6]:-

$$F' = \frac{h_1 h_{r,p-c} + h_2 U_t + h_2 h_{r,p-c} + h_1 h_2}{(U_t + h_{r,p-c} + h_1)(U_b + h_2 + h_{r,p-c}) - h_{r,p-c}^2} \quad \dots (26)$$

Collector heat removal factor is given by [6]:-

$$F_R = \frac{\dot{m} C_p}{A_c U_L} \left[1 - e^{-\left(\frac{A_c U_L F'}{\dot{m} C_p}\right)} \right] \quad \dots (27)$$

The actual useful energy gain of the hot air in the collector can be calculated by the equation below [6]:-

$$Q_u = A_c F_R [S - U_L \Delta T] \quad \dots (28)$$

Then the collector efficiency which represents the indicator to its performance can be given by:-

$$\eta_c = \frac{Q_u}{A_c I_T} \quad \dots (29)$$

2.2. Mathematical Model in the Chimney

The hot air which is less denser than ambient air by overcoming the gravity and friction start rising from the chimney [7], the chimney efficiency is given as [9]:-

$$\eta_{ch} = \frac{P_{tot}}{Q_u} = \frac{gH_{ch}}{C_p T_a} \quad \dots (30)$$

where, H_{ch} is the height of the chimney, thus the power contained in the flow P_{tot} from equation (31) can be expressed as follows [9]:-

$$P_{tot} = \eta_{ch} Q_u = \frac{gH_{ch}}{C_p T_a} Q_u \quad \dots (31)$$

Q_u is the actual useful energy gain can be obtained from equation (28).

A pressure difference Δp is produced between chimney base (collector outflow) and the surroundings [9]:-

$$\Delta p = \rho_a g H_{ch} \frac{\Delta T}{T_a} \quad \dots (32)$$

3. Numerical Simulation

The numerical simulation includes simulation of solar chimney using ANSYS FLUENT (version14.0). ANSYS-FLUENT is a computer package used for modeling fluid flow and heat transfer in complex geometries, the present study carried out FLUENT (version 14.0) to solve continuity, momentum, and energy, equations using a finite volume method. For the simulations, steady state analysis was chosen. The working fluid used was air which was modeled as an ideal gas. The buoyancy model was activated by specifying the gravity of -g in the (y) direction which represented real life flow. The reference pressure used was 1atm.

3.1 Modeling Geometry

- i. The geometry creation is done by the Solid works (2013) software program. In the coordinate (x) and (z) are in the radial directions, and (y) is in the vertical direction.
- ii. In this model using the mesh sizing Relevance center type fin and from mesh inserting element size equal=0.0275m[10] with set the mesh shape triangle. The mesh of reduction area is shown in Fig.(5).

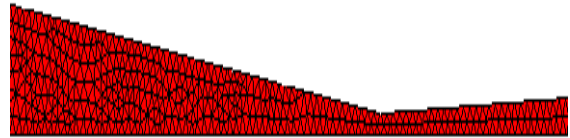


Fig. 5. Mesh of reduction area for the solar chimney model.

3.2 Numerical Setup

i. Setting Model

In the present simulations, the basic settings of the fluent simulation are by activated the energy equation, select the Realizable k- ϵ full buoyancy effects in the viscous model to describe the fluid flow inside the collector and the chimney, and select the discrete ordinate (DO) radiation model to solve the radiation transfer equation for the following reasons, first only the DO model can be used to model semi-transparent walls, and second the DO model can work well across a full range of optical thicknesses.

ii. Setting Materials properties

Table 1, Physical properties of materials [11].

Physical property	Air	Glass roof	Chimney wall	Ground	Insulation
Density kg/m ³	1.167	2700	7833	2719	24
Thermal Conductivity W/mK	0.0242	0.78	54	202.4	0.038
Specific heat J/kg K	1006.43	840	465	871	700
Refractive index [-]	1	1.526	1	1	1
Emissivity [-]	-	0.9	-	0.94	-
Thermal Expansion Coefficient 1/K	0.0033	-	-	-	-

iii. Boundary Conditions

Table 2, Boundary conditions of the physical model.[12]

Boundary	Type	Parameter value
Collector inlet	Pressure inlet	$T = T_a$, $p = 1\text{atm}$
Chimney outlet	Pressure outlet	$T = T_a$, $p = 1\text{atm}$
Absorbing plate	Wall	Convection + Radiation
Glass roof	Wall	Convection + Radiation
Chimney	Wall	Fixed heat flux $q = 0$

4. Experimental Work

The simulation model with six fold collector and chimney is used in The experimental study. The diameter of collector and chimney (4.5m,20cm) respectively[13], chimney’s height is 4m, collector is inclined at 2.3°with inlet of collector is 4cm [14]. The absorption ground of collector made from black aluminum with thickness 1mm. The reduction area means that change of height of glass cover from the absorption plate at the defined distance from the center of solar chimney model .The aim from using reduction area the effect of it on air velocity. The design velocity that enters the chimney . From the simulation taken three different height of reduction area $h1=3.8\text{cm}$, $h2=2.6\text{cm}$ and $h3=1.28\text{cm}$. making comparative with experimental work as shows in Figure(6):

Distance of reduction area from the center of collector
Radius of collector

$$\frac{2.43}{4.10} = 0.59 \quad [3] \quad \dots (33)$$

$$\frac{A}{2.25} = 0.59 \leftrightarrow A = 1.33\text{m}$$

A:-distance of reduction area from the center of collector. And height of reduction area calculated same the calculated the far of reduction area about the center. The distance A and B shown in fig.(7b)

$$\frac{\text{Height of reduction area}}{\text{Height collector inlet}} = \frac{0.16}{0.50} 0.32 \quad [3] \quad \dots (34)$$

$$\frac{B}{0.04} = 0.32 \leftrightarrow B = 0.0128$$

B:-height of reduction area (h3)in experimental work. h2 and h1 is triple and double h3 respectively.. The Scale model of solar chimney power plant and reduction area shown in figure (6),(7 a,b) respectively.



Fig. 6. Scale model of solar chimney power plant.



Fig. 7a. The position of reduction area.

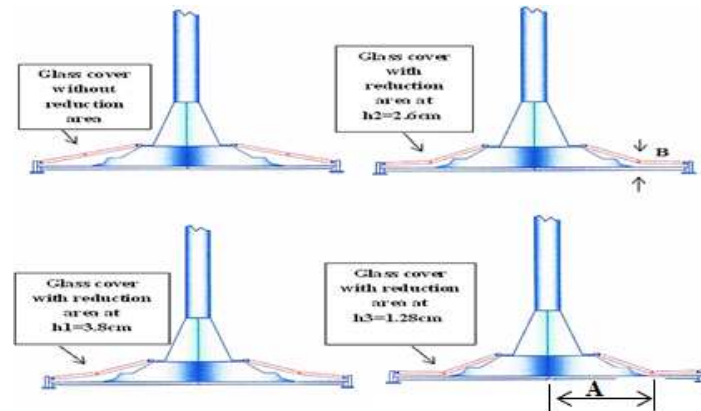


Fig. 7b. Schematic diagram of shape of glass cover for the consider cases.

4.1. Instrumentations

The following section describes the measuring instruments used on the experimental. The data are recorded every 1 hour. Fig (8) shows the different instrumentations used in this work. The solar meter model 776 is hand solar intensity meter was used to measure solar flux. This model is ideal for measuring the solar energy absorbed by a flat panel collector. Has the photovoltaic cell located on the front of the meter body so it can be placed flat on the surface and the measurement read directly from the scale. The air velocity at the chimney entrance was measured by metal van anemometer model (YK-80AM). The velocity measurement range starts from (0.4) and reach to (35) m/s and temperature range (0 to 60 C°) including record function captures and displays minimum and maximum reading. The LCD shows air velocity and temperature reading simultaneously. Data logger model BTM-4208SD has been used to record temperature data. 12 channels of thermocouples have been connected to this data acquisition system. Data is saved on the SD card and can be transferred to a PC and analyzed. Surface temperature of the collector cover (agricultural nylon) was measured using infrared thermometer model AR300. The

temperature measurement range (32 to 400 C°). It offers LCD backlight for visibility in the dark, a broad temperature range, and a dual display for both current and maximum measurements. Five points are located on the collector cover divided along it with 39 cm distance between each one. The first point begins at 4 cm from inlet of collector. This distribution is constant in all cases. Ten thermocouples K-type were used to measure the ambient temperature, absorber plate and air temperature inside the solar chimney. The thermocouples and its locations are defined as follows.

- Five thermocouples are located on the absorber plate divided along it with 39 cm distance between each one. The first thermocouple begins at 4 cm from inlet of collector. This distribution is constant in all cases.
- Five thermocouples are located in the flow direction of air to measure air temperature. These thermocouples are divided along air flow direction with 52 cm distance between each one.

All data are automatically collected and recorded in a PC through data logger. The positions of the thermocouples are as shown in Fig. (9).



Fig. 8. Photographic view of the instrumentation.

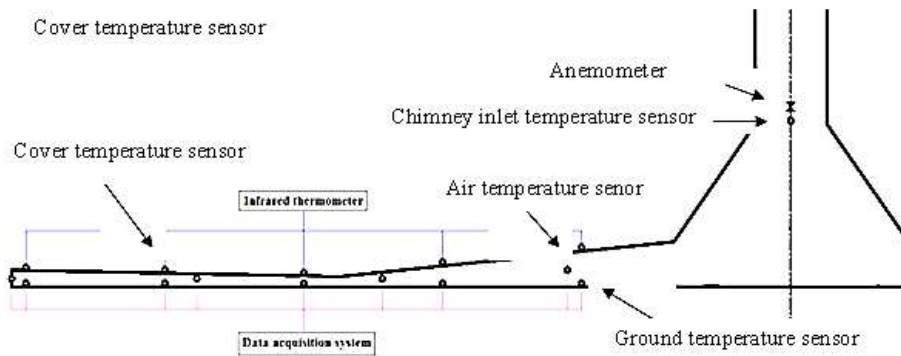


Fig. 9. Layout of thermocouples and data collecting points.

5. Results and Discussions

Case studies of experimental works were taken in May month at Baghdad city under actual weather conditions of this month. The experimental data had collected from 9 AM to 2 PM. Fig. (10a) presents the behavior of the airflow velocity experimentally at the inlet chimney tower with time at various collector reduction areas. The highest velocity occurs at 1:00PM, when the levels of incident solar radiation and the airflow temperatures are higher. Higher values are found at the lower collector reduction area. For the prototype with the collector reduction area 3.8 cm, the maximum achievable velocity is 2.55 m/s at 1:00PM. By decreasing the collector reduction area to 1.28 cm, the maximum achieved velocity rises to 3.15 m/s which is about an 19.04% enhancement. A lower collector reduction area means a smaller collector flow area, giving a higher airflow velocity.

Fig. (10b) shows the variation of air velocity with time among inclination angle and reduction area of collector. It is noticed that air velocity corresponding to reduction area $h=1.28$ cm is higher than that to inclination angle 2.3° resulting from the reduction of flow area. by decreasing the collector reduction area, the maximum achieved velocity rises from 2.39 m/s to 3.15 m/s which is about an 24.12% enhancement, the airflow temperature inside the solar collector increased with respect to the solar radiation intensity (I). It is also observed that the airflow temperature at $h_3=1.28$ cm of the solar collector is higher than those at $h_1=3.8$ cm, and $h_2=2.6$ cm during the whole testing period. Fig. (14) illustrates the history of airflow temperature, for three different values of the collector reduction areas. Higher collector reduction area reduces the airflow temperature due to the increase of the mass flow

rate. Mass flow rate increased by increasing flow area in the collector.

The maximum absorber ground temperature recorded at 1:00PM was 65°C , where the collector cover temperature reached the value of 43°C and the air temperature was 40°C these results for inclination angle of collector (2.3°) fig.(14a). While for collector reduction area ($h_3=1.28$ cm), the maximum absorber ground temperature was 93°C , the collector cover temperature was 67°C and the air temperature was 62°C . The comparison showed that the reduction area was more effective than that inclination angle fig (14b).

Fig.(11a) demonstrates the evolution of output power versus time for three different values of the collector reduction area. This figure illustrates that the output power increases while the collector reduction area is decreased. Current result predict higher output power with collector reduction area of $h=1.28$ cm than a plants with a collector reduction area of $h=3.8$ cm and $h=2.6$ cm. The output power for reduction area of (1.28cm) is observed higher than that for inclination angle of collector of 2.3° shown in fig.(11b), because it is the effect of lower reduction area in collector. it can be observe the collector efficiency ($\frac{\dot{m}c_p \Delta T}{Ac I}$) increases as the reduction area of the collector decreases due to its higher outlet temperature and airflow velocity. Fig. (12a) demonstrates that the collector efficiency increases from 29% to 51% according to the decrease in collector areas from $h_1=3.8$ cm to $h_3=1.28$ cm.

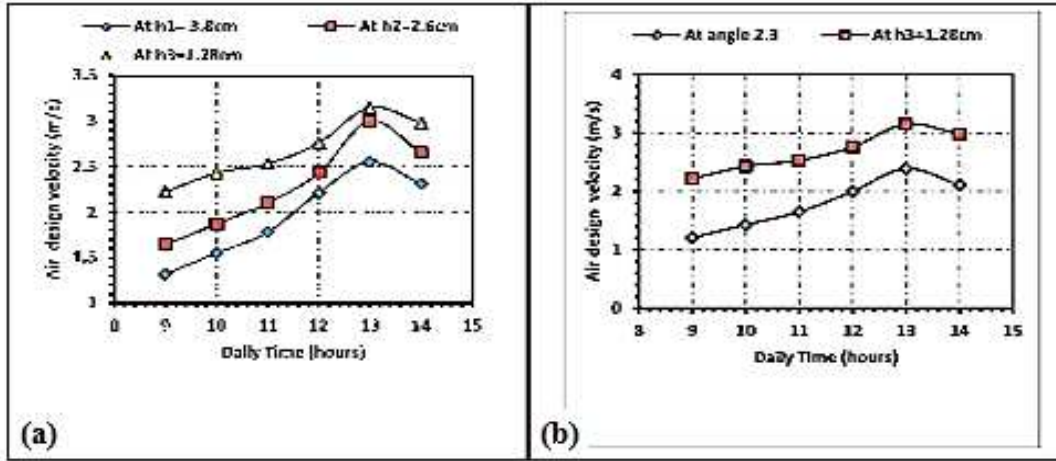


Fig. 10. Variation of air velocity versus time (a)with reduction area. (b) with and without reduction area.

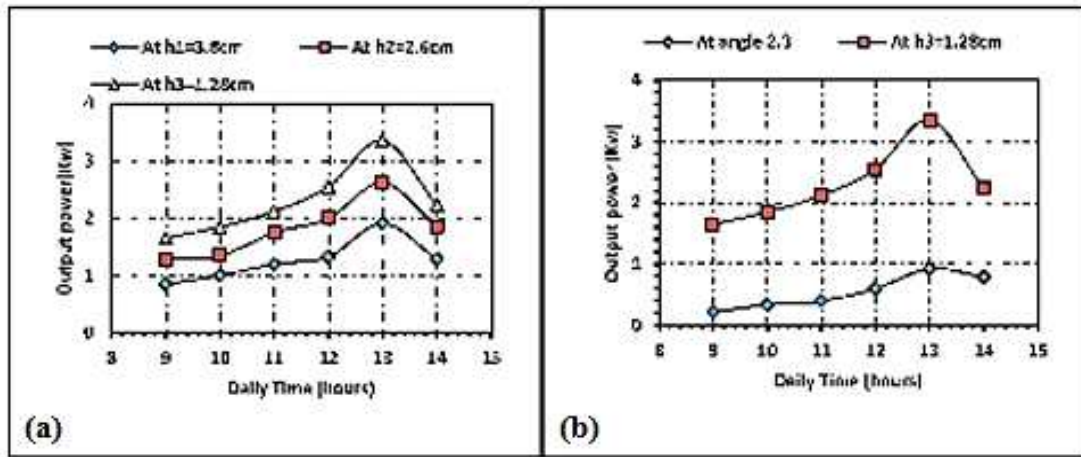


Fig. 11. Variation output power versus time (a)with reduction area.(b)with and without reduction area.

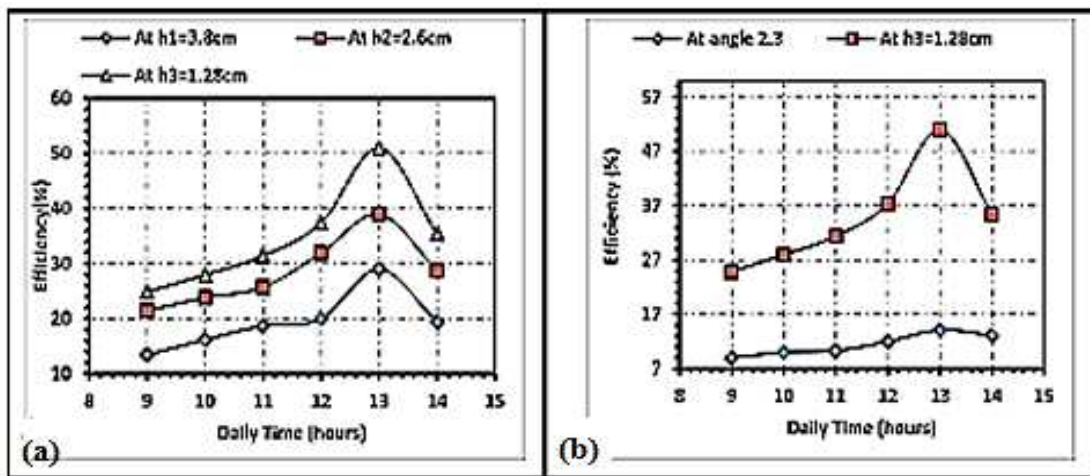


Fig. 12. Variation efficiency versus time(a) with reduction area. (b) with and without reduction area.

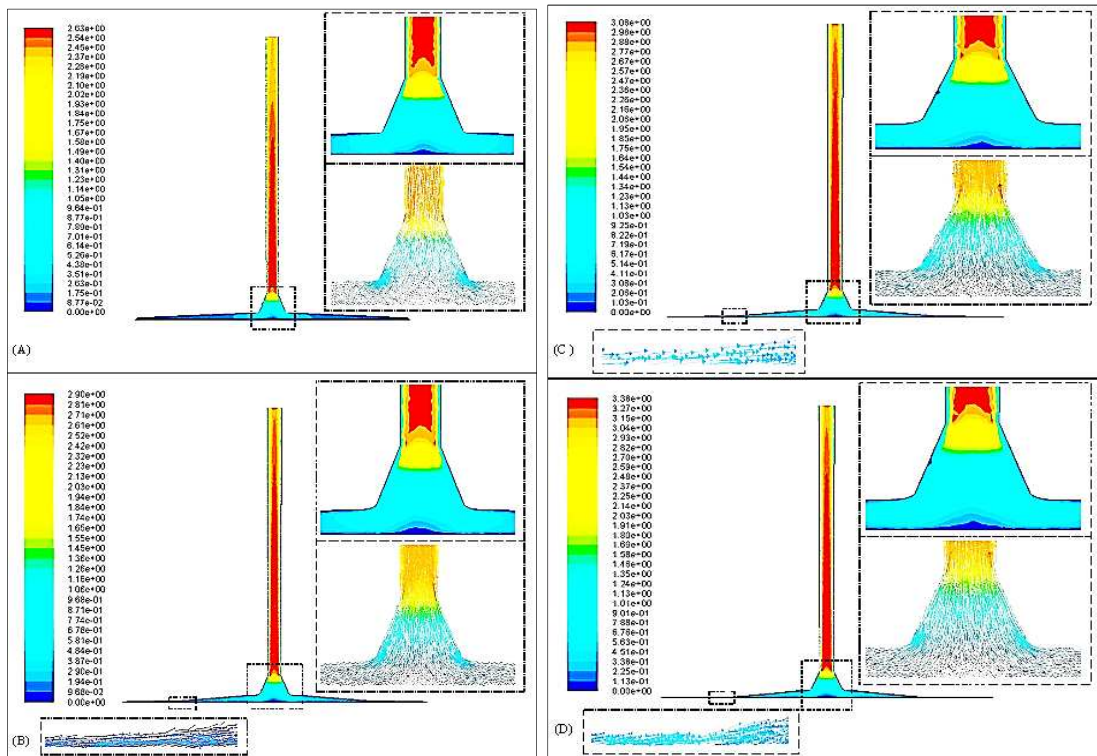


Fig. 13. Contours and vectors of air design velocity (m/s) (A) without reduction area. (B) at $h_1=3.8\text{cm}$. (C) at $h_2=2.6\text{cm}$. (D) at $h_3=1.28\text{cm}$.

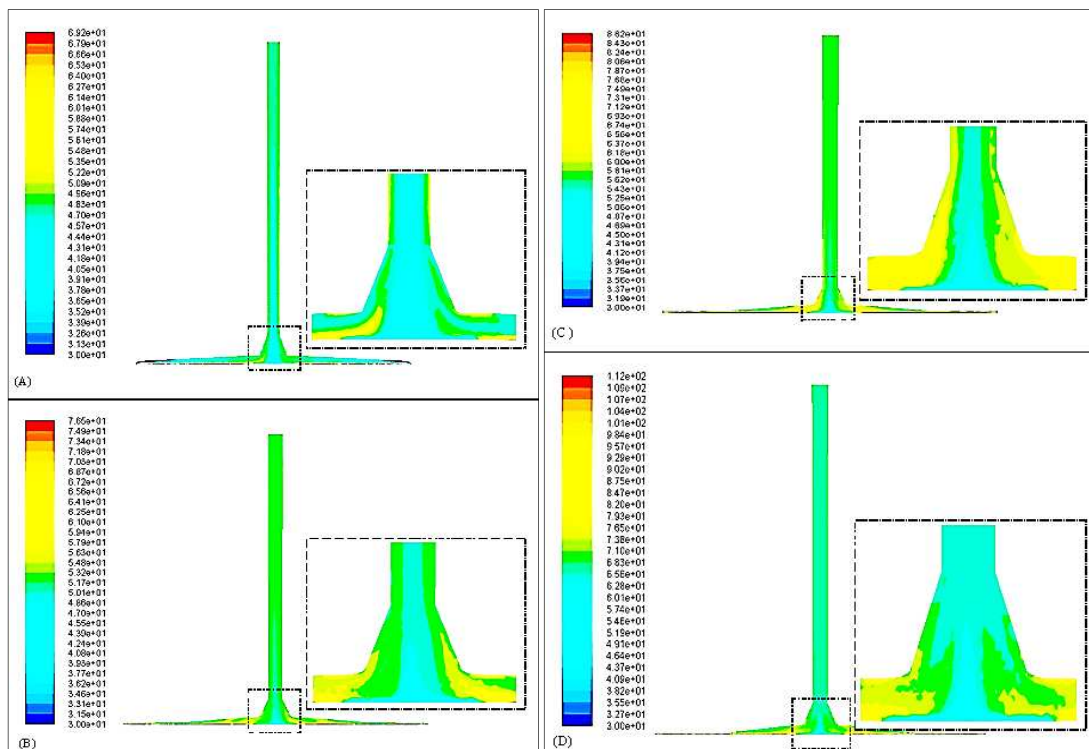


Fig. 14. Contours of static air temperature (c°) (A) without reduction area. (B) at $h_1=3.8\text{cm}$. (C) at $h_2=2.6\text{cm}$. (D) at $h_3=1.28\text{cm}$.

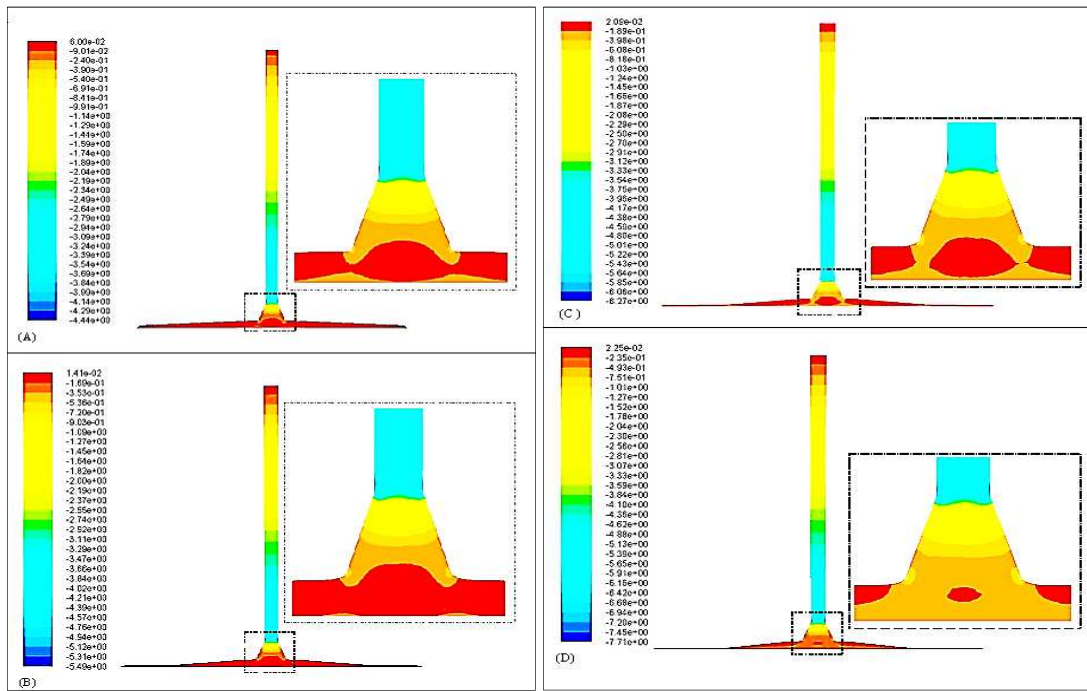


Fig. 15. Contours of static pressure(pa) (A)without reduction area.(B)at h1=3.8cm.(C) at h2=2.6cm. (D) at h3=1.28cm.

6. Conclusions

According to the discussion of the obtained results, many conclusions can be extracted such as:-

1. The effects of three different collector reduction areas on solar chimney are presented. It can be concluded that decreasing the collector reduction area significantly influences on the performance of solar chimney. In the present study, collector reduction area of 1.28 cm provides the best performance.
2. The collector inclination angle is also important parameter in the solar chimney. The inclination angle of collector should be at optimum angle to provide best performance for solar chimney.
3. The reduction area is found to perform better than an inclination angle in terms of airflow velocity and temperature.
4. The thermal efficiency of the solar collector is dependent upon the magnitude of temperature rise (ΔT) and the airflow velocity, and also of the solar radiation.

Error Analysis

When experimental tests are carried out, an accurate reading should be taken, since any mistakes could reduce the accuracy of the results.

There is more than one method which can be used to find the experimental error. One of these methods is that given by: Kline & Melintock [11] which depends on the assumption that when calculating a variable as R for example, which is to be calculated from a certain experimental test. This variable is assumed to be related to a number of independent variables as ($v_1, v_2... v_n$)

$$R = R(v_1, v_2, \dots, v_n) \quad \dots(35)$$

For small variations in the variables, this relation can be expressed in linear form as:

$$\delta R = \frac{\partial R}{\partial v_1} \delta v_1 + \frac{\partial R}{\partial v_2} \delta v_2 + \dots + \frac{\partial R}{\partial v_n} \delta v_n \quad \dots(36)$$

Hence, the uncertainty intervals (w) in the result can be given as

$$w_R = \left[\left(\frac{\partial R}{\partial v_1} w_1 \right)^2 + \left(\frac{\partial R}{\partial v_2} w_2 \right)^2 + \dots + \left(\frac{\partial R}{\partial v_n} w_n \right)^2 \right]^{1/2} \quad \dots(37)$$

Eq. (38) is greatly simplified upon dividing by Eq. (36) to non-dimensionalize

$$\left(\frac{w_R}{R}\right)^2 = \left(\frac{\partial R}{\partial v_1} \frac{w_1}{R}\right)^2 + \left(\frac{\partial R}{\partial v_2} \frac{w_2}{R}\right)^2 + \dots + \left(\frac{\partial R}{\partial v_n} \frac{w_n}{R}\right)^2 \dots(38)$$

Hence, the experimental errors that may happen in the used variables are given in Table (3) for the measuring devices;

**Table 3,
Uncertainties of Measuring Tools.**

Independent Variables (V)	Uncertainty Interval (W)
Temperature	0.2 °C
Velocity	0.02
Solar intensity	0.02

Error in calculating the value of collector efficiency

$$\eta_c = \frac{C_p \rho_T V_T A \Delta T}{I 3 \frac{\sqrt{3}}{2} R_c^2} \dots (39)$$

Collector efficiency is a functional of several variables, each subject to an uncertainty.

$$\eta_c = f(V_T, \Delta T, I) \dots (40)$$

$$\frac{\partial \eta_c}{\partial \Delta T} = \frac{C_p \rho_T V_T A}{I 3 \frac{\sqrt{3}}{2} R_c^2} \dots (41)$$

$$\frac{\partial \eta_c}{\partial V_T} = \frac{C_p \rho_T A \Delta T}{I 3 \frac{\sqrt{3}}{2} R_c^2} \dots (42)$$

$$\frac{\partial \eta_c}{\partial I} = \frac{C_p \rho_T A V_T \Delta T}{I^2 3 \frac{\sqrt{3}}{2} R_c^2} \dots (43)$$

Therefore the uncertainty intervals (w) in the result can be given as follows;

$$W_{\eta_c} = \left[\left(\frac{\partial \eta_c}{\partial \Delta T} W_{\Delta T} \right)^2 + \left(\frac{\partial \eta_c}{\partial V_T} W_{V_T} \right)^2 + \left(\frac{\partial \eta_c}{\partial I} W_I \right)^2 \right]^{\frac{1}{2}} \dots (44)$$

$$\frac{W_{\eta_c}}{\eta_c} = \frac{0.15428}{68} = 0.00226 \%$$

7. References

[1] Schlaich Bergermann und Partner, “Solar updraft tower”, October 2011 <http://www.solar-updraft-tower.com>.
 [2] Mark E.Steinke,Satish G.Kandlikar, “Single-phase heat transfer enhancement techniques

in microchannel and minichannel flows”, AZME,2004.

[3] Atit Koonsrisuk, “Analysis of flow in solar chimney for an optimal design purpose”, thesis, 2009.
 [4] Hermann F. Fasel, Fanlong Meng, Ehsan Shams, Andreas Gross, “CFD analysis for solar chimney power plants”, Solar Energy 98 (2013) pp. (12–22).
 [5] Qahtan A. Al-Nakeeb, “Computational analysis of geometry alteration on the performance of a solar system to generate air flow”,thesis, Iraq, 2001.
 [6] Duffie, John A. and Beckmann, William A. (1980), “Solar Engineering of Thermal Processes”, book, John Wiley & Sons, New York.
 [7] M.A. dos S. Bernardes, A. Voß, G. Weinrebe, “Thermal and technical analyses of solar chimneys”, Solar Energy 75 (2003) pp. (511–524).
 [8] Mehrdad Ghalamchi, Alibakhsh Kasaeian, “An experimental study on the thermal performance of solar chimney with different dimensional parameters” ,Volume 91, 2016, pp. (477–483).
 [9] Roozbeh Sangi, “Performance evaluation of solar chimney power plants in Iran”, Renewable and Sustainable Energy Reviews 16 ,(2012), pp. (704– 710).
 [10] Abbas Jassem Jubear Abbas, “Numerical and experimental study of turbine - solar chimney performance”,thesis, Iraq, (2014).
 [11] J.P. Holman, Heat Transfer 5th edition, book ,McGraw-Hill, 1981.
 [12] ANSYS Fluent 12.0 user’s guide and theory guide.
 [13] Bashir Ahmed Danzomo, Sani Jibrin, “Similitude model design and performance evaluations of solar tower system”, ARPN Journal of Engineering and Applied Sciences, VOL. 7, NO. 4, 2012.
 [14] Haider Salim Nuri, “Enhancement of solar chimney performance by using geometrical and thermal energy storage techniques”, thesis, 2014.

دراسة عملية وعددية لتأثير شكل المجمع على إداء المدخنة الشمسية

أسيل خليل شياع*
 رافع عباس حسن البنداوي**
 مريم مؤيد عبود***

*قسم الهندسة الميكانيكية/ الجامعة التكنولوجية
 البريد الإلكتروني: aseelkhshyaa@yahoo.com
 **البريد الإلكتروني: rafa_a70@yahoo.com
 ***البريد الإلكتروني: memomoaed@yahoo.com

الخلاصة

تطورت محطات التوليد الكهربائية بواسطة المدخنة الشمسية منذ سنة 1930م. محطة الطاقة الشمسية تعد مولدا للطاقة النظيفة. الدراسة الحالية هي عملية وعددية عن منطقة الانخفاض في المجمع الشمسي. منطقة الانخفاض تعني تغير الارتفاع بين سقف المجمع الشمسي وبين صفيحة الامتصاص (قاع المجمع الشمسي) التي تكون ذات بعد معين عن مركز المجمع وهذا البعد يعتمد على حجم النودج المستعمل. دُرِسَ تغير ارتفاعات منطقة الانخفاض عمليا وعدديا حيث تم استخدام ثلاثة ارتفاعات (3.8، 2.6، 1.28) سم على التوالي. الهدف من هذا البحث هو دراسة تأثير ارتفاعات منطقة الانخفاض على سرعه التصميمية (السرع الذي تقوم بتحريك ريش التوربين الموجودة عند مدخل المدخنة). بينت النتائج ان استخدام الارتفاع 1.28 سم هو الافضل والسبب في ذلك عند تقليل الارتفاع بين السقف والقاع تعني تقليل من مساحه الجريان داخل المجمع الشمسي مما يؤدي الى زياده في سرعه الجريان تؤدي الى زياده كفاءة المدخنة الشمسية.